Dielectrophoresis of air

Cite as: Appl. Phys. Lett. **116**, 084101 (2020); https://doi.org/10.1063/5.0002286 Submitted: 23 January 2020 . Accepted: 12 February 2020 . Published Online: 25 February 2020

Lucas Soffer 📵, Abigail Rendos 📵, Aleksandrs L. Zosuls 📵, Brian M. Walsh 📵, and Keith A. Brown 📵







ARTICLES YOU MAY BE INTERESTED IN

Quantum dot arrays in silicon and germanium

Applied Physics Letters 116, 080501 (2020); https://doi.org/10.1063/5.0002013

Wideband detection of electromagnetic signals by high-T_C Josephson junctions with comparable Josephson and thermal energies

Applied Physics Letters 116, 082601 (2020); https://doi.org/10.1063/1.5142400

Light-induced transition between the strong and weak coupling regimes in planar waveguide with GaAs/AlGaAs quantum well

Applied Physics Letters 116, 081102 (2020); https://doi.org/10.1063/1.5141362





Dielectrophoresis of air

Cite as: Appl. Phys. Lett. 116, 084101 (2020); doi: 10.1063/5.0002286 Submitted: 23 January 2020 · Accepted: 12 February 2020 · Published Online: 25 February 2020



















AFFILIATIONS

- ¹Department of Mechanical Engineering, Boston University, Boston, Massachusetts 02215, USA
- ²Division of Materials Science and Engineering, Boston University, Boston, Massachusetts 02215, USA
- ³Biomedical Engineering Department, Boston University, Boston, Massachusetts 02215, USA
- Electrical and Computer Engineering Department, Boston University, Boston, Massachusetts 02215, USA
- Center for Space Physics, Boston University, Boston, Massachusetts 02215, USA
- ⁶Physics Department, Boston University, Boston, Massachusetts 02215, USA

ABSTRACT

Dielectrophoresis describes neutral particles moving in non-uniform electric fields. We experimentally observe the dielectrophoresis of gas generated by macroscopic electrodes and show that this effect can be large enough to generate audible sound. The observed sound agrees with a multiscale model of dielectrophoresis of gas. The compositional dependence of this effect is shown through experiments on mixtures of nitrogen and carbon dioxide, as well as volatile molecules in air.

Published under license by AIP Publishing. https://doi.org/10.1063/5.0002286

Electrically polarizable objects experience a force due to the interaction between their induced dipole and non-uniform electric fields, which was coined dielectrophoresis (DEP) in 1951. Applications of DEP have ranged from separating polar and non-polar molecules in liquids, sorting colloidal particles, 1,3,4 filtering dust particles out of air,⁵ pumping or mixing non-conductive liquids,^{6,7} and repelling bubbles to facilitate boiling heat transfer. More recently, DEP has found tremendous use in the biological and microfluidic realms⁹ where it is routinely used to manipulate cells, 10,11 nanoparticles, 12-15 and biomolecules. 16,17 While our understanding of DEP is evolving due to an emerging appreciation for the importance of permanent dipoles, 18, these applications are widespread because the DEP force is typically proportional to the volume of an object, resulting in appreciable forces for microscale objects in the presence of modest electric fields.²⁰ The same scaling, however, makes it difficult to observe DEP on smaller objects such as individual molecules. Nevertheless, in an ideal gas, each gas molecule should experience a minute force pulling it toward regions of high field intensity. As the system will rapidly relax to local thermodynamic equilibrium, such forces will increase the gas pressure by $p_a \alpha E^2/2k_BT$ with molecular electrical polarizability α , atmospheric pressure p_a , local electric field E, Boltzmann's constant k_B , and temperature T (Fig. 1). Since $\alpha \sim 10^{-40} \text{ C} \cdot \text{m}^2/\text{V}$ for an individual molecule,^{23,24} the fractional increase in local pressure for E = 5 kV/cm, which is below the $\sim 30 \text{ kV/cm}$ threshold for dielectric breakdown of air, 25,26 is only predicted to be $\sim 10^{-8}$ (corresponding to

an \sim 1 mPa absolute pressure shift). Despite the fact that this is miniscule, humans can perceive $\sim 10^{-10}$ fractional pressure shifts, suggesting that the DEP-induced pressure shifts could be large enough to be audible.²⁷ Thus, if one considers applying an alternating current (AC) electric field, the pressure shift will oscillate at twice the frequency of the applied AC signal and potentially give rise to propagating sound

In this paper, we observe the DEP of ambient gas in the presence of macroscopic electric fields. By constructing macroscopic electrode arrays and measuring the sound produced by these arrays, we observe sound at a frequency that is characteristic of the electrode geometry and that has an amplitude that agrees with a continuum model of DEP of gas. In order to prove that this sound originates from DEP, we repeat these experiments with mixtures of carbon dioxide and nitrogen and find the magnitude and frequency of emitted sound to be in agreement with analytical predictions. Additionally, we find that ethanol or isopropanol vapors in air produce predictable and discernable acoustic signatures when driven using DEP. Having shown that electrodes behave as coherent sources of sound by applying DEP forces directly on gas molecules, we test a set of concentric ring electrodes that are designed to produce sound that coherently converges at a specified focal point and experimentally demonstrate that DEP-generated sound is intense enough to be audible and can be created in a spatially complex fashion using acoustic sources that are substantially sub-wavelength.

^{a)}Authors to whom correspondence should be addressed: brownka@bu.edu and bwalsh@bu.edu

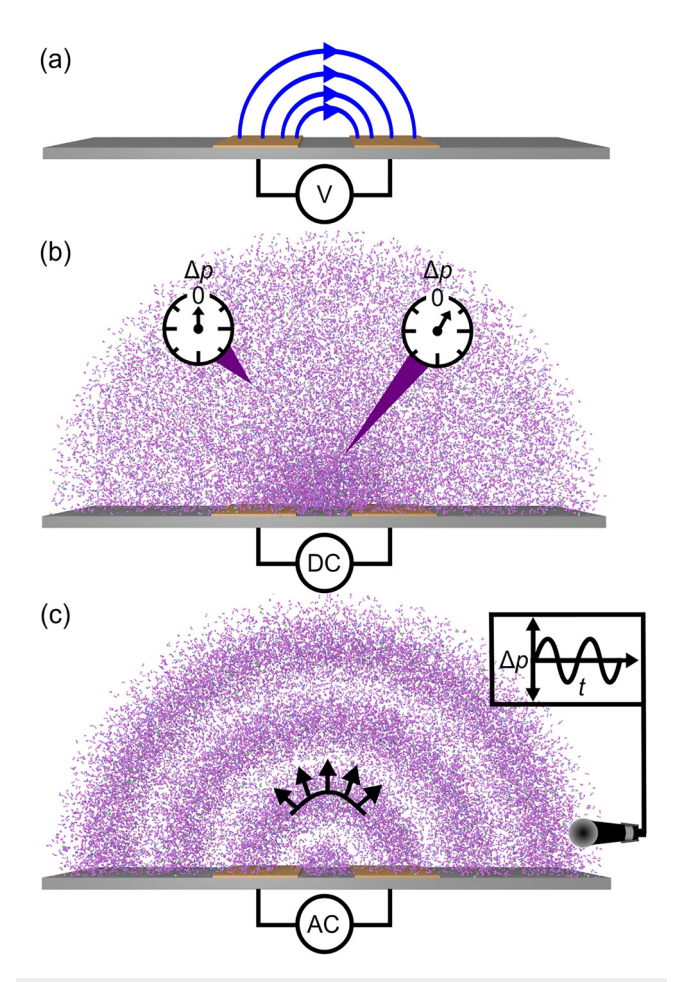


FIG. 1. (a) In the vicinity of energized electrodes, electrically neutral gas molecules experience an electrostatic force acting on their induced dipoles. (b) Even though DEP is substantially weaker than thermal fluctuations, it will produce a slight positive pressure shift Δp in the high field region. (c) An oscillating electric field produces an intermittent attractive force that leads to pressure oscillations that propagate away from the electrodes.

In order to test the hypothesis that DEP can give rise to appreciable sound, we designed an electrode array to function as an array of acoustic sources. The electric field produced by parallel strip electrodes was found using electrostatic finite element analysis [Fig. 2(a)]. In order to understand the effect this field would have on proximal gas, the compressible Navier-Stokes equations and continuity were used as governing equations in which DEP was included as a body force. These equations can either be directly solved numerically or linearized in the acoustic limit and solved using Green's functions (supplementary material). 28,29 Using either approach, we found that the high field region between the electrodes was expected to produce sound oscillating at twice the frequency of the applied field that propagates in a cylindrically symmetric fashion (i.e., a two dimensional field with axial symmetry) [Figs. 2(b) and S1]. With this insight in hand, the gap between a pair of electrodes can be considered an acoustic line source with a magnitude and phase determined by the details of the driving voltage and the ambient gas. Importantly, this lumped element approach allows the behavior of an array of line sources to be rapidly calculated to determine the conditions under which such an array will produce a coherent beam of sound propagating along the surface of the board [Figs. 2(c) and S3].

Having predicted that a linear electrode array should be capable of producing sound, we performed a series of experiments to measure the sound produced by an interdigitated series of electrodes. Experiments were carried out in an audiometric test room (IAC Acoustics) in which a printed circuit board was driven at frequency f with a root-mean-squared voltage V and observed using a proximal microphone [Fig. 2(d)]. The board consisted of 53 electrode pairs with a periodicity L = 5 mm, which were driven at V = 40 V using a high voltage amplifier (PA98-Apex Microtechnology). Sound was measured using a microphone (Type 4138-Brüel & Kjaer), amplified by 20 dB using a microphone amplifier (Type 5935—Brüel & Kjaer), and then input into a lock-in amplifier (Model SR830-Stanford Research Systems) to select the 2f component of the signal. To measure the pressure amplitude p_0 , a 10 min collection time was used with a 30 s lock-in integration time constant with a 12 dB slope. By sweeping f, p_0 was mapped, revealing a peak frequency $f_R = 34.8 \,\mathrm{kHz}$ [Fig. 2(e)]. According to our model of DEP-generated sound, this resonant frequency is determined by the geometry of the electrode array, namely, $f_R = c_0/(2L)$ with sound speed c_0 . The high noise present at 50 kHz is reflective of operating at the upper bandwidth limit of our lock-in amplifier. After identifying f_R , p_0 at $f = f_R$ was measured vs V and fit to $p_0 = aV^2$ [Fig. 2(f)] to find $a = 2.0 \pm 0.1$ nPa/V², which is similar to the 4 nPa/V² theory prediction for an array with infinitely long electrodes (supplementary material). In order to further verify that this signal corresponded to sound and not a direct electrical coupling between the board and the microphone, the phase φ of this signal was measured as the microphone was moved along the surface of the board [Fig. 2(g)]. As anticipated, φ increased linearly as the microphone moved in the direction of the acoustic beam, confirming that the measured signal was due to sound propagating in air. While the observed sound is in quantitative agreement with DEP, we also performed a series of experiments evaluating other mechanisms including thermoacoustic sound generation and electrostriction of the solid support, both of which were unable to match the observed data (supplementary material). Corona wind—or the sustained motion of gas that arises from sustained corona discharge—has been previously used to generate sound but uses much larger voltages (> kV) than present here and in a direct current (DC) configuration, rather than the \sim 40 V alternating current voltages used in the present study. 30,31

It is important to note that the voltages used here are substantially lower in frequency than the molecular dielectric resonances exhibited by gases in air (e.g., $60\,\mathrm{GHz}$ for $\mathrm{O_2}$). Thus, α can be approximated as purely real and constant with respect to frequency. Correspondingly, the resonant conditions of a given electrode array originate from its geometry and not the dielectric properties of the gas. Looking beyond the present study, the increase in α at frequencies near molecular dielectric resonances suggests that operation at high frequencies commensurate with these resonances could provide a chemically specific path to efficiently manipulate gas molecules.

Since DEP depends on the properties of the gas, we hypothesized that changing the gas composition would change DEP-generated sound in an observable fashion. To explore this, we developed an experiment to measure DEP-generated sound in a sealed enclosure in

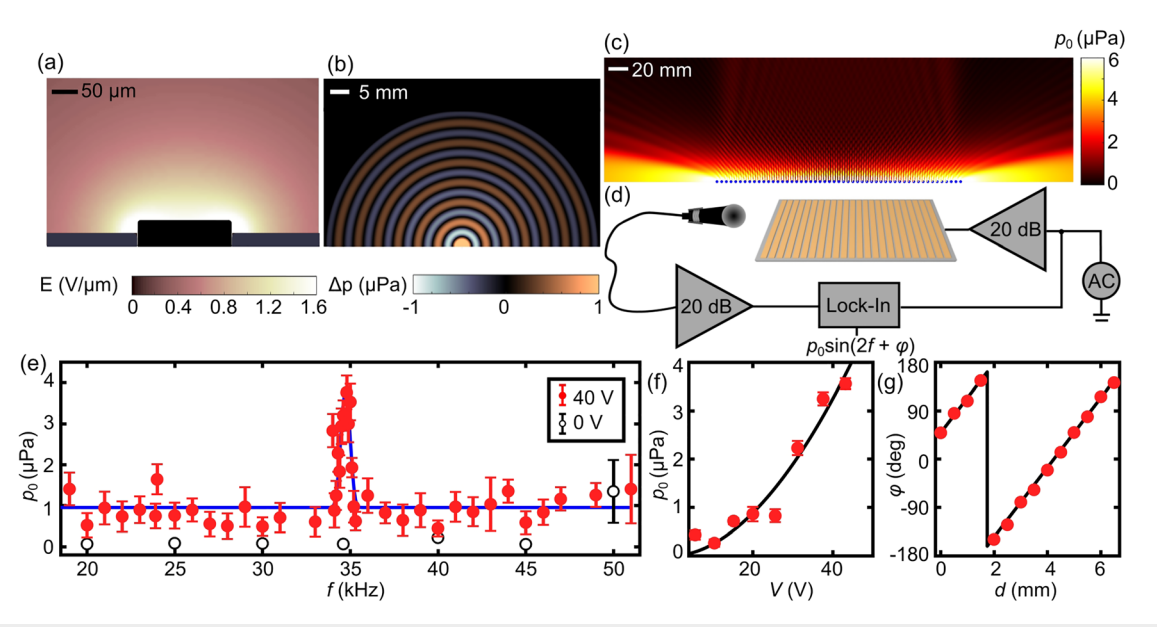


FIG. 2. (a) A cross section of the local electric field E is peaked in the region between two electrodes. (b) If E oscillates at frequency f, compressible fluid flow computation reveals that the change in pressure Δp propagates radially away from the gap between the electrodes. (c) The pressure wave amplitude p_0 produced by an electrode array with blue dots corresponding to the gaps between electrodes. (d) Schematic of the experimental system used to detect sound produced by a linear electrode array. (e) Experimentally measured p_0 in the vicinity of a linear electrode array driven with applied voltage V = 40 V (red) or 0 V (black). (f) Measured p_0 at f = 34.8 kHz. (g) Pressure wave phase p_0 measured vs microphone position p_0 with p_0 and p_0 and p_0 are p_0 at p_0 at p_0 at p_0 and p_0 are p_0 at p_0 at p

which we could control the gas composition. Our model predicts that for a given electrode array, a and f_R would depend on α and c_0 , respectively. Specifically, we sought to explore the DEP-induced sound in CO_2 , for which α is 50% higher than N_2 , the principal component of air. Initially, the sound generated by the electrode array with $V=40\,\mathrm{V}$ was measured in air [Fig. 3(a)]. Without moving any components of the system or changing any settings, the enclosure was purged with

pure CO_2 . After allowing the system to equilibrate for 30 min, the f sweep experiment was repeated. Importantly, the shift in f_R confirms that the gas had been replaced with CO_2 due to the slower c_0 in CO_2 relative to that in air. More importantly, however, is that p_0 at f_R increased. To test the generality of this effect, we repeated this experiment with 2:1 $CO_2:N_2$ and 1:2 $CO_2:N_2$ and observed the same trend with p_0 at f_R decreasing concomitantly with the CO_2 composition.

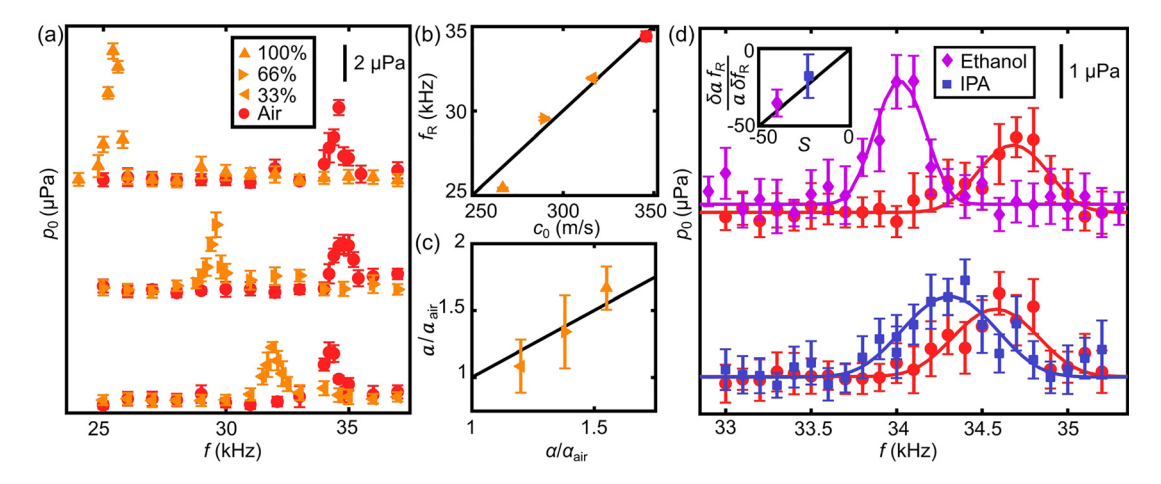


FIG. 3. (a) Measurements of sound produced by a linear electrode array in a sealed enclosure with a controlled gas environment. Measurements with a set percentage of CO_2 in a host gas of N_2 (orange) are compared with measurements in air (red) taken with the system in the same configuration. (b) Predicted speed of sound c_0 vs experimental resonance frequency f_R . (c) Ratio of the pressure coefficient a registered for the CO_2 – N_2 mixture relative to that of air a_{air} , vs the ratio of the average polarizability α of the CO_2 – N_2 mixture relative to that of air α_{air} . (d) Measurements of p_0 produced by a linear electrode array in a sealed enclosure with air (red) and a vapor of ethanol (purple) or isopropyl alcohol (IPA—blue). The inset shows experimentally determined relative pressure shift $\delta a/a$ relative to sound speed shift $\delta f_R/f_R$ vs DEP sensitivity factor S, which is calculated from material properties.

Critically, f_R [Fig. 3(b)] and a [Fig. 3(c)] calculated for each composition agree with the theoretical model of DEP generated sound. Being based upon the continuous flow of purified gases, there was minimal water vapor present in the atmosphere, an important fact considering that water has a strong dipole moment.

While observing that acoustic generation is proportional to α lends proof to the proposed model for DEP-generated sound, we sought to explore whether small quantities of volatile molecules could appreciably change DEP-generated sound. Thus, we performed a series of experiments in which p_0 vs f was measured in an air-filled chamber and then again in the same chamber after introducing a small container of liquid ethanol or isopropanol (IPA); both liquids that have large α, non-zero molecular dipole moments, and substantial vapor pressures at room temperature. Upon exposure to a vapor of either liquid, f_R decreased and a increased [Fig. 3(d)]. These experiments provide evidence that DEP-generated sound can encode chemical information in both the speed and magnitude of sound. In particular, the p_0 of DEP-generated sound increased relative to p_0 in air by 67% in the presence of ethanol and by 14% in the presence of IPA. To understand this, we performed a perturbation analysis of p_0 and c_0 in the presence of an arbitrary analyte species (supplementary material). While the relative shift in either quantity depends on the concentration of the analyte present, the ratio of the fractional shift in p_0 to the fractional shift in c_0 is invariant of concentration. Thus, we compare this experimentally measured value to a DEP sensitivity factor S, which depends only on material properties (Table S3 and supplementary material), and find agreement between theory and experiment [inset of Fig. 3(d)], in further support of DEP being the mechanism of sound generation. Importantly, α for a material with a static dipole moment must include this static dipole in a thermalized fashion.

Having shown that electrodes on printed circuit boards can produce a significant enough DEP force on gas to generate observable sound, we sought to explore the degree to which arrays of electrodes could produce more complex acoustic profiles and whether these can be audible. Considering the region of the high field between electrodes to be an acoustic line source, we hypothesized that controlling the position and phase of such electrodes could allow one to realize a phased array of acoustic sources for controlling the magnitude and direction of sound. This is an empowering concept because deep sub-wavelength electrodes can be constructed with a high degree of complexity on printed circuit boards with small and scalable drive electronics. Thus, to explore this concept, we designed a set of concentric ring electrodes [Fig. 4(a)]. This electrode array, when driven at f= 10 kHz, is expected to behave as a zone plate in which the signal produced by all electrodes constructively interferes at one location along the central axis. Directly computing the expected pressure field produced by this array gives rise to a well-defined pressure maximum at a point 10 cm away from the board [Fig. 4(b)]. In contrast, the pressure field predicted when the board is driven off resonance at $f = 15 \,\mathrm{kHz}$ is substantially weaker and lacks the maximum at 10 cm [Fig. 4(c)]. A ring electrode array board was produced and tested in an audiometric test room to find p_0 along the center axis, while it was driven with a 10 kHz signal with V = 193 V [Fig. 4(c)]. A clear maximum was detected at the expected focal point with a maximum pressure of ~4 mPa, corresponding to a definitively audible signal when compared to the human auditory threshold.²⁷ This experiment was

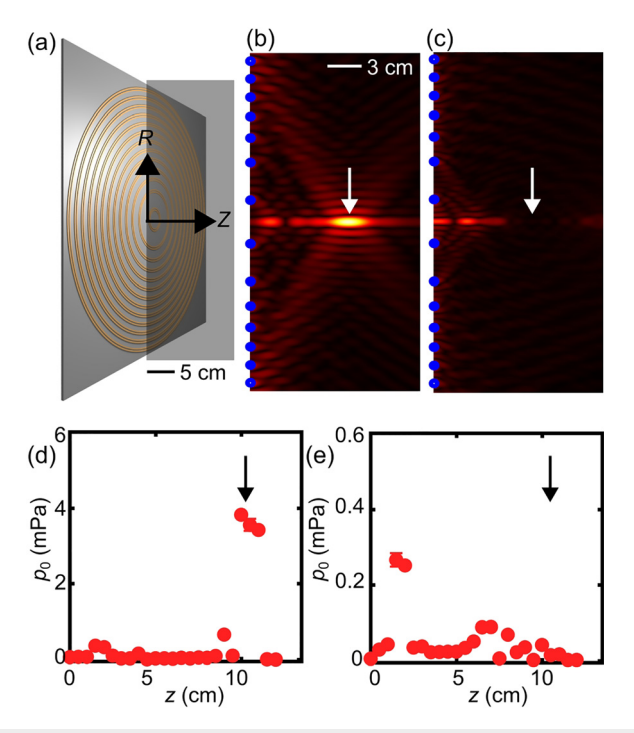


FIG. 4. (a) Schematic of the zone plate composed of a series of concentric ring electrodes. Computed pressure field produced by the zone plate operating at (b) $f=10~\mathrm{kHz}$ and (c) $f=15~\mathrm{kHz}$. Blue dots correspond to the location of electrode pairs. Experimentally measured p_0 vs axial distance z at (d) $f=10~\mathrm{kHz}$ and (e) 15 kHz. The arrows highlight the expected focal point when driven on resonance (10 kHz), which, as expected, shows a peak in (b) and (d) and the absence of a peak in (c) and (e).

repeated at 15 kHz, and as expected, a maxima was not observed at 10 cm as the frequency did not match the coherence conditions.

While the study of DEP has evolved in >60 years since its discovery, the observation that macroscopic electrodes and modest voltages can produce audible sound illustrates that there remain fundamental discoveries to be made. In light of recent work highlighting the importance of permanent dipoles in DEP interactions, ^{18,19} the quantification of molecular dipole moments through acoustic methods could provide important tools for the development of more complete theories of DEP. Agreement between experiment and theory confirms that the observed phenomenon is due to DEP and provides a framework for predicting the acoustic generation from arbitrary electrode arrangements. Due to the simplicity of the experimental setup and low cost of printed circuit boards, the barrier for follow-on work is low. While the magnitude of DEP generated sound is small, the fact that audible sound can be realized using modest voltages and macroscopic electrodes indicates that it may be present in other settings, perhaps playing a role in the audible noise caused by transmission lines, which is currently analyzed in an empirical manner and known to have a spectral peak at twice the frequency of the voltage.^{35–37} As the active elements that generate sound can be substantially sub-wavelength, produced as part of standard printed circuit board fabrication, and feature no moving parts, they are highly amenable for developing active metamaterials or phase-controlled antenna array applications.

See the supplementary material for additional details regarding methods, a derivation of DEP-generated sound, a multiscale calculation of DEP-generated sound, a derivation of DEP of air with volatile additives, and discussion of potential alternate explanations of the observed sound.

This work was supported by the National Science Foundation (No. CMMI-1661412). We also acknowledge the support through the Boston University Photonics Center and the Boston University Undergraduate Research Opportunities Program. Acknowledgment is made to the donors of the American Chemical Society Petroleum Research Fund for the support of this research through Award No. 57452-DNI9. A.R. acknowledges support from a BUnano Cross-Disciplinary Fellowship. We acknowledge helpful discussions with Professor R. Glynn Holt.

REFERENCES

- ¹H. A. Pohl, J. Appl. Phys. 22(7), 869–871 (1951).
- ²G. Karagounis, Nature **161**(4100), 855 (1948).
- ³H. A. Pohl and J. Schwar, J. Appl. Phys. **30**(1), 69–73 (1959).
- ⁴H. A. Pohl and J. P. Schwar, J. Electrochem. Soc. 107(5), 383-385 (1960).
- ⁵L. Silverman, E. W. Conners, and D. Anderson, Ind. Eng. Chem. 47(5), 952–960 (1955).
- ⁶H. A. Pohl, J. Appl. Phys. **29**(8), 1182–1188 (1958).
- ⁷W. Cropper and H. Seelig, Ind. Eng. Chem. Fundam. 1(1), 48–52 (1962).
- ⁸M. Markels and R. L. Durfee, AIChE J. **10**(1), 106–110 (1964).
- ⁹R. Pethig, Biomicrofluidics 4(2), 022811–022835 (2010).
- ¹⁰H. A. Pohl and I. Hawk, Science **152**(3722), 647–649 (1966).
- ¹¹B. H. Lapizco-Encinas, B. A. Simmons, E. B. Cummings, and Y. Fintschenko, Anal. Chem. 76(6), 1571–1579 (2004).
- ¹²S. Hermanson, S. O. Lumsdon, J. P. Williams, E. W. Kaler, and O. D. Velev, Science 294, 1082 (2001).

- ¹³B. H. Lapizco-Encinas and M. Rito-Palomares, Electrophoresis 28(24), 4521–4538 (2007).
- ¹⁴K. A. Brown and R. M. Westervelt, Nano Lett. **11**(8), 3197–3201 (2011).
- ¹⁵W. Cao, M. Chern, A. M. Dennis, and K. A. Brown, Nano Lett. 19(8), 5762–5768 (2019).
- ¹⁶C.-F. Chou, J. O. Tegenfeldt, O. Bakajin, S. S. Chan, E. C. Cox, N. Darnton, T. Duke, and R. H. Austin, Biophys. J. 83(4), 2170–2179 (2002).
- ¹⁷P. Modarres and M. Tabrizian, Sens. Actuators, B 252, 391-408 (2017).
- ¹⁸R. Pethig, Electrophoresis **40**(18–19), 2575–2583 (2019).
- ¹⁹D. V. Matyushov, Biomicrofluidics **13**(6), 064106 (2019).
- ²⁰A. T. J. Kadaksham, P. Singh, and N. Aubry, Electrophoresis 25(21–22), 3625–3632 (2004).
- ²¹I. Ermolina and H. Morgan, J. Colloid Interface Sci. 285, 419–428 (2005).
- ²²A. Castellanos, A. Ramos, A. González, N. G. Green, and H. Morgan, J. Phys. D: Appl Phys. 36, 2584–2597 (2003).
- ²³P. Schwerdtfeger, in Atoms, Molecules and Clusters in Electric Fields: Theoretical Approaches to the Calculation of Electric Polarizability (World Scientific, 2006), pp. 1–32.
- ²⁴P. T. Van Duijnen and M. Swart, J. Phys. Chem. A **102**(14), 2399–2407 (1998).
- ²⁵W. S. Boyle and P. Kisliuk, Phys. Rev. **97**(2), 255 (1955).
- ²⁶A. Wallash and L. Levit, Proc. SPIE **4980**, 87 (2003).
- ²⁷M. C. Killion, J. Acoust. Soc. Am. **63**(5), 1501–1508 (1978).
- ²⁸J. M. Eargle, in *Handbook of Recording Engineering* (Springer, 1996), pp. 1–37.
 ²⁹P. M. Morse and K. U. Ingard, *Theoretical Acoustics* (Princeton University
- 30 S. Park, U. Cvelbar, W. Choe, and S. Y. Moon, Nat. Commun. 9(1), 371 (2018).
- ³¹D. Tombs, Nature **176**(4489), 923–923 (1955).
- ³²P. Rosenkranz, Absorption of microwaves by atmospheric gases (John Wiley and Sons, 1993).
- 33V. V. Daniel, Dielectric Relaxation (Academic Press, 1967).
- ³⁴B. Ma, J. H. Lii, and N. L. Allinger, J. Comput. Chem. **21**(10), 813–825 (2000).
- 35 Z. Engel and T. Wszołek, Appl. Acoust. 47(2), 149-163 (1996).
- ³⁶V. Chartier and R. Stearns, IEEE Trans. Power Appar. Syst. PAS-100(1), 121–130 (1981).
- ³⁷X. Bian, L. Chen, D. Yu, J. MacAlpine, L. Wang, Z. Guan, F. Chen, W. Yao, and S. Zhao, IEEE Trans. Dielectr. Electr. Insul. 19(6), 2037–2043 (2012).